PHYSICAL REVIEW E **79**, 030601(R) (2009)

Quantitative phase-field modeling of solidification at high Lewis number

J. Rosam,[1,2] P. K. Jimack,[2] and A. M. Mullis[1]
[1]*Institute for Materials Research, University of Leeds, Leeds LS2-9JT, United Kingdom*
[2]*School of Computing, University of Leeds, Leeds LS2-9JT, United Kingdom*

(Received 22 August 2008; revised manuscript received 17 December 2008; published 12 March 2009)

A phase-field model of nonisothermal solidification in dilute binary alloys is used to study the variation of growth velocity, dendrite tip radius, and radius selection parameter as a function of Lewis number at fixed undercooling. By the application of advanced numerical techniques, we have been able to extend the analysis to Lewis numbers of order 10 000, which are realistic for metals. A large variation in the radius selection parameter is found as the Lewis number is increased from 1 to 10 000.

DOI: 10.1103/PhysRevE.79.030601 PACS number(s): 68.70.+w, 81.30.Fb, 02.60.Cb, 64.70.dm

INTRODUCTION

The growth of dendritic structures during solidification has been a subject of enduring interest within the scientific community, both because it is a prime example of spontaneous pattern formation and due to the pervasive influence of dendrites on the engineering properties of metals. As dendrites are self-similar when scaled against the tip radius ρ, the ability to accurately predict ρ is a problem of central importance to the theory of dendritic growth.

However, the prediction of ρ has proved exceptionally challenging. Early analytical solutions [1] predicted that it was the dimensionless Peclet number $\mathrm{Pe}=V\rho/2D$ (V=growth velocity, D=diffusivity in the liquid) that was related to undercooling, ΔT, during growth, leading to a degeneracy in the product $V\rho$ not observed in nature. Various models based on the stability of planar solidification fronts were proposed [2,3] to break this degeneracy, although ultimately the application of boundary integral methods established that it is crystalline anisotropy [4] rather than stability *per se* that is responsible for breaking the degeneracy. The analysis reveals that in the limit of vanishing Pe an equation similar to that arising from stability arguments is recovered, but with a radius selection parameter σ^* that varies as $\varepsilon^{7/4}$, where ε is the anisotropy strength.

In recent years significant progress toward understanding solidification processes has also been afforded by the advent of phase-field modeling. However, the application of phase-field modeling has largely been restricted to two limiting cases: namely, the thermally controlled growth of pure substances and the solidification of relatively concentrated alloys (e.g., [5]) where growth is sufficiently slow that the problem may be considered isothermal. However, this omits alloy solidification problems where the isothermal approximation is not valid, specifically the solidification of very dilute alloys and rapid solidification processes.

To date, relatively few attempts have been made to use phase-field techniques to simulate coupled thermosolutal solidification due to the severe multiscale nature of the problem (typically the Lewis number $\mathrm{Le}=\alpha/D$ is 10^3-10^4, where α is the thermal diffusivity). Loginova *et al.* [6] have developed a coupled model using a derivation based on the solutal model of Warren and Boettinger [7], although there are doubts about the quantitative validity of this model [8] as the numerical results appear to suggest excess solute trapping and have an unresolved interface width dependence. This methodology has been extended by Lan *et al.* [9], who introduced an adaptive finite-volume solver, which allowed them to use realistic values of Le, although this did not overcome either the excess solute trapping or the interface-width dependence of the solution. An alternative formulation of the coupled phase-field problem has been presented by Ramirez and Beckermann [8,10], based on the Karma [11] thin-interface model. As the thin-interface model has been shown to be independent of the length scale chosen for the mesoscopic diffuse interface width, it is capable of giving quantitatively correct predictions for dendritic growth, although Ramirez and Beckermann only used the model at relatively modest Lewis numbers (typically 40).

In a previous paper [12] we used a fully implicit, adaptive finite-difference implementation of the model due to [8] to investigate the dependence of ρ upon ΔT at $\mathrm{Le}=200$, demonstrating that ρ passes through a minimum with increasing ΔT, as predicted by stability models such as that due to Lipton, Kurz, and Trivedi [3] (LKT). We also showed that the radius selection parameter, σ^*, not only varies with ΔT, but that the variation is nonmonotonic.

In this paper we now consider the extent to which ρ, V, and σ^* vary as Le is increased at fixed ΔT. This quantitative analysis of the Lewis number dependence has previously been considered in [8], albeit in the restricted range $1 \leqslant \mathrm{Le} \leqslant 200$, wherein it was found that the predictions of the LKT [3] theory were valid for $\mathrm{Le} \leqslant 5$, with significant deviations thereafter. Here we extended the analysis to higher values of Le, including values up to 10^4, which are of appropriate order for metals, in which dendritic growth is most common.

DESCRIPTION OF THE MODEL

The model adopted here is based upon that of [8] in which, following nondimensionalization against characteristic length and time scales W_0 and τ_0, the evolution of the phase field ϕ and the dimensionless concentration and temperature fields U and θ are given by

$$A^2(\psi)\left[\frac{1}{\mathrm{Le}} + Mc_\infty[1+(1-k_E)U]\right]\frac{\partial\phi}{\partial t}$$
$$= \nabla\cdot[A^2(\psi)\nabla\phi] + \phi(1-\phi^2) - \lambda(1-\phi^2)^2(\theta + Mc_\infty U)$$
$$- \frac{\partial}{\partial x}\left(A(\psi)A'(\psi)\frac{\partial\phi}{\partial y}\right) + \frac{\partial}{\partial y}\left(A(\psi)A'(\psi)\frac{\partial\phi}{\partial x}\right),$$

$$\left(\frac{1+k_E}{2} - \frac{1-k_E}{2}\phi\right)\frac{\partial U}{\partial t}$$
$$= \nabla\cdot\left(D\frac{1-\phi}{2}\nabla U + \frac{1}{2\sqrt{2}}|1+(1-k_E)U|\frac{\partial\phi}{\partial t}\frac{\nabla\phi}{|\nabla\phi|}\right)$$
$$+ \frac{1}{2}\left(|1+(1-k_E)U|\frac{\partial\phi}{\partial t}\right),$$

$$\frac{\partial\theta}{\partial t} = \alpha\nabla^2\theta + \frac{1}{2}\frac{\partial\phi}{\partial t},$$

where, for fourfold growth, $A(\psi)=1+\varepsilon\cos(4\psi)$, d_0 is the chemical capillary length, k_E is the partition coefficient, L and c_p are the latent and specific heats, respectively, and λ is a coupling parameter given by $\lambda=D/a_2=a_1W_0/d_0$, with a_1 and a_2 taking the values $5\sqrt{2}/8$ and 0.6267, respectively [11]. U and θ are related to physical concentration c and temperature T via

$$U = \frac{1}{1-k_E}\left[\left(\frac{2c/c_\infty}{1+k_E-(1-k_E)\phi}\right) - 1\right]$$

and

$$\theta = \frac{\Delta T - mc_\infty}{L/c_p},$$

where m is the slope of the liquidus line, which has dimensionless form

$$M = \frac{|m|(1-k_E)}{L/c_p}.$$

The governing equations are descritized using a finite-difference approximation based upon a quadrilateral, nonuniform, locally refined mesh with equal grid spacing in both directions. This allows the application of standard second-order central difference stencils for the calculation of first and second differentials, while a compact nine-point scheme has been used for Laplacian terms, in order to reduce the mesh induced [13] anisotropy. To ensure sufficient mesh resolution around the interface region and to handle the extreme multiscale nature of the problem at high Lewis number, local mesh refinement (coarsening) is employed when the weighted sum of the gradients of ϕ, U, and θ exceeds (falls below) some predefined value.

It has been shown elsewhere that if explicit temporal descretization schemes are used for this problem, the maximum stable time step is given by $\Delta t \leqslant Ch^2$, where $C=C(\lambda,\mathrm{Le},\Delta T)$, with C varying from ≈ 0.3 at Le=1 to $C \leqslant 0.001$ at Le=500 [14], leading to unfeasibly small time steps at high Lewis number. Consequently, an implicit temporal descretization is employed here based on the second-order backward difference formula with variable time step.

When using implicit time discretization methods, it is necessary to solve a very large, but sparse, system of nonlinear algebraic equations at each time step. Multigrid methods are among the fastest available solvers for such systems, and in this work we apply the nonlinear generalization known as the full approximation scheme (FAS) [15]. The local adaptivity is accommodated via the multilevel algorithm originally proposed by Brandt [16]. The interpolation operator is bilinear, while injection is used for the restriction operator. For smoothing the error we use a fully coupled nonlinear weighted Gauss-Seidel iteration where the number of pre- and post-smoothing operations required for optimal convergence is determined empirically [14]. Full details of the numerical scheme are given in [12,14,17].

RESULTS

To explore the effect of Lewis number on V and ρ, the model has been run at a fixed undercooling of $\Delta=0.15$ over a wide range of Lewis numbers from 1 to 10 000, the latter being the typical order for metals. A coupling parameter of $\lambda=5$ has been adopted in all simulations, and in order to simulate kinetic free growth via the relation $\lambda=D/a_2$, we set $D=3.1335$, which also fixes the interface width of $\approx 5.6d_0$. The required variation in Le is effected by varying α. All other material and computation parameters were held constant across all simulations. We have taken $\varepsilon=0.02$, which is widely used for the anisotropy strength of many metals, while k_E and Mc_∞ have been taken as 0.3 and 0.05, respectively, these being typical of the alloy Cu–5 wt % Ni (for Cu-Ni, we have at Cu-rich compositions $k_E \approx 0.3$, $|m|=6.2$ K/wt %, and $L/c_p \approx 430$ K [18], giving $M=0.01$/wt % and $\Delta T=65$ K). The minimum grid spacing of $h=0.78$ is held constant across all simulations, although the size of the domain is varied such that there is no interaction between the thermal field and the domain boundary. The largest domain used was $\Omega=[-3200,3200]^2$, wherein 13 levels of refinement are required to achieve the desired h. This is equivalent, were a uniform mesh to have been used, of a mesh size of $2^{13}\times 2^{13}$. This compares with our previously reported largest equivalent grid [12] of $2^{12}\times 2^{12}$ with therefore correspondingly longer run times.

We obtain from the model the two key parameters characteristic of dendritic growth: namely, the velocity and radius of the tip. The latter we obtain by fitting a parabolic profile to the $\phi=0$ isoline using a fourth-order interpolation scheme described in [14,12], as this has generally been felt [8,19] to be more directly comparable to analytical dendrite growth theories [3] than the curvature directly from the derivatives of ϕ at the tip. From empirical trials we estimate the error associated in determining ρ from the parabolic fitting process to be around $\pm 4\%$.

The dependence of V and ρ on Le is shown, in dimensionless form, in Figs. 1 and 2, respectively (dimensional values for the Cu–5 wt % Ni example system can be obtained by taking $D \approx 3.2\times 10^{-9}$ m^2 s^{-1} [20] and $d_0=3.7\times 10^{-10}$ m [18]). For both ρ and V, we may delineate high- and low-Le

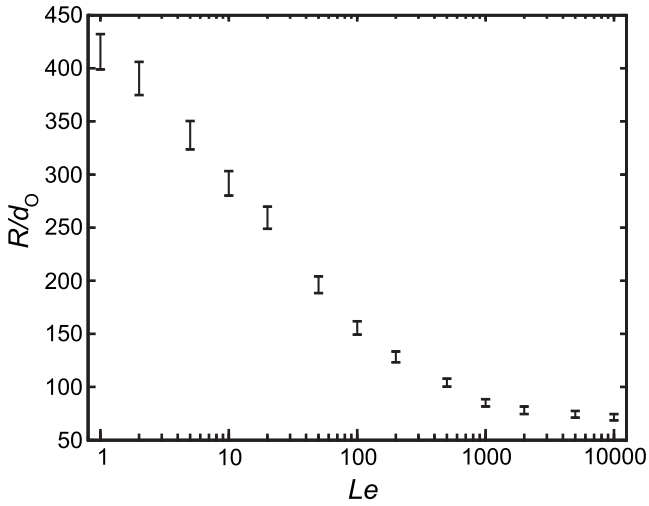

FIG. 1. Calculated variation of the dimensionless radius of curvature at the tip as a function of Lewis number.

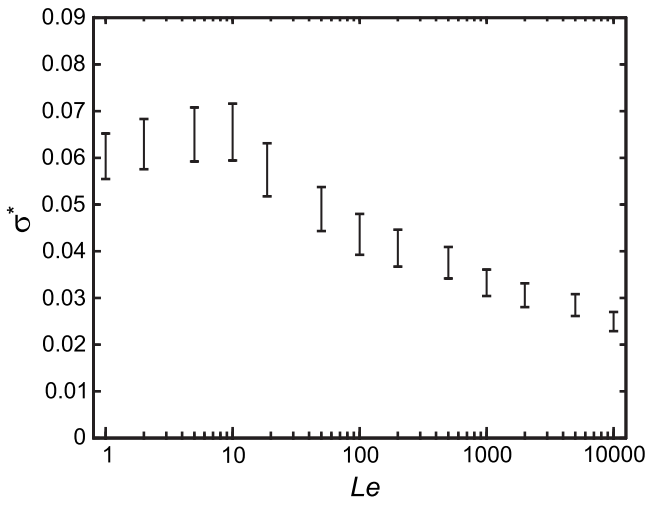

FIG. 3. Calculated variation of the radius selection parameter σ^* as a function of Lewis number.

behavior, with this boundary occurring around Le=1000. For high Lewis numbers, ρ is essentially independent of Le with a logarithmic dependence at low Le. At the lowest values of Le studied (<5), there is possibly a trend toward a leveling off again, although this has not been investigated as there is no significance for values of Le<1. Relative to the results found by [8], we observe a much larger variation in ρ over the comparable range of Lewis numbers (to Le=200 [8] observed ρ to drop by ~30% of its Le=1 value, whereas we observe a 67% drop). We attribute this to the fact that we have conducted our investigation at much lower undercooling, which is consistent with LKT predictions of ρ as a function of Le (see, e.g., Fig. 6 in Ref. [12]).

At low Lewis numbers, Vd_0/D varies, to a good approximation, as a simple power law with an exponent close to 2.5, leveling off somewhat in the high-Lewis-number regime, although unlike ρ, V continues to increase with Lewis number up to the highest values studied. For comparison with [8] we have also shown Vd_0/α which as in [8] shows little variation

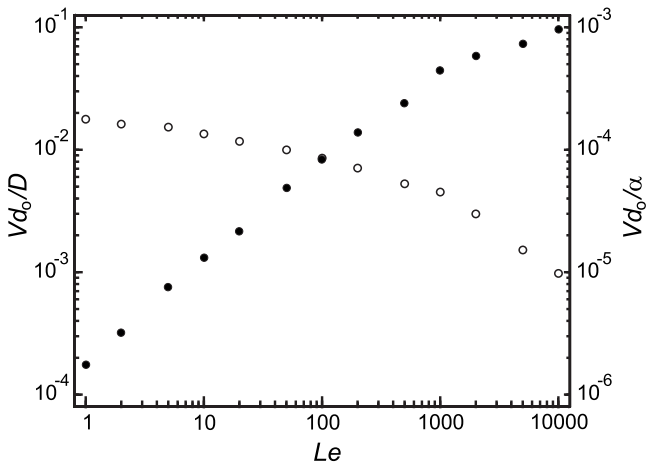

FIG. 2. Calculated variation of the dimensionless tip velocity as a function of Lewis number (left-hand scale and solid markers nondimensionalized against d_0/D, right-hand scale, and open markers against d_0/α).

over the range $1 \leqslant \mathrm{Le} \leqslant 200$ (note, however, that the scaling factor d_0/α is dependent on Le).

In addition to V and ρ, an important auxiliary quantity that may be calculated is the radius selection parameter σ^*. Following the methodology proposed in [8], we evaluate σ^* based on the LKT [3] definition, where the supersaturation at the interface is evaluated without reference to the Ivantsov [1] solution by considering U_i, the value of U "frozen in" at the interface (taken as $\phi=0$). The resulting variation of σ^* with Le is shown in Fig. 3, where the error shown is ±8% (based on ±4% error in ρ with σ^* varying as $1/V\rho^2$). At low Lewis number, σ^* may initially show a slight increase with increasing Le, although the errors associated with determining σ^* are such that the results would also be consistent with σ^* being constant, which is as found by [8] at similar Lewis numbers. In the limit of Lewis number of unity, we find that $\sigma^*=0.0604$, in very close agreement with the value found in [8]. We find that this value is, as noted in [8], also close to that for a dendrite growing under solute only control [the coupled model can be used for solute only growth at solutal undercooling Ω by fixing the system temperature everywhere at $\theta_{sys}=-\Omega$ with $Mc_\infty=1-(1-k_E)\Omega$ (see [14])].

For Le>10 we find, in agreement with [8], that the assumption of constant σ^* breaks down. However, at high Δ ($\Delta=0.55$) [8] found that σ^* (LKT definition) first decreased slightly before increasing markedly as Le is increased. In contrast, we find that at $\Delta=0.15$, beyond Le=10, σ^* decreases monotonically with increasing Lewis number, dropping to ~0.025 at Le=10 000. This represents a variation of around a factor of 3 over the range of Le studied.

SUMMARY AND DISCUSSION

We have used a phase-field model of nonisothermal solidification in dilute binary alloys to study the variation of V, ρ, and σ^* as a function of Lewis number at fixed undercooling. By using advanced numerical techniques such as mesh adaptivity, implicit time stepping, and multigrid methods, we have been able to extend the analysis to Lewis numbers of

order 10 000, these values being typical of metallic systems. Moreover, the formulation of the nonisothermal problem based on the thin-interface model which we have adopted from [8] means that these results should be independent of the width assumed for the diffuse interface, giving them a quantitative validity which cannot be claimed by formulations of the problem not based around the thin-interface model, such as [6,9]. We find that the tip radius ρ drops monotonically with increasing Le, becoming almost constant at high Le with a value in this case close to $70d_0$, while V increases monotonically with increasing Le, reaching a value of $\sim 0.1 d_0/D$ at the highest values of Le studied. For the example system of Cu–5 wt % Ni this would correspond to a dimensional growth velocity (the primary quantity measured during rapid solidification experimentation (see, e.g., [21,22]) of 0.9 m s^{-1}, although direct comparison with experiment is not possible as two- and three-dimensional solidifications are quantitatively different. For the radius, and to a lesser extent the tip velocity, qualitatively different behavior is seen in what we may define as the low-Lewis-number regime ($\mathrm{Le} < 1000$) to that in the high-Lewis-number regime, and this value therefore defines a minimum level at which simulations may be classed as approaching "realistic" for metallic systems. This transition, albeit rather gradual, presumably delineates which of the two transport processes is dominant.

The radius selection parameter σ^* has been calculated as a function of Le, and a variation of a factor of 3 is observed over the range of Lewis numbers studied. This further highlights the potential limitations of assuming constant σ^* in analytical models of solidification to predict dendrite length scales. Moreover, for $\mathrm{Le} > 10$, σ^* decreases monotonically with increasing Le, raising an apparent contradiction as in the limit $\mathrm{Le} \to \infty$ the dendrite should return to fully solutal control and the value of σ^* appropriate to the solute-only model should be recovered. In both this and previous studies [12,14], the model has produced results in close agreement with other authors (for $\mathrm{Le} \leqslant 200$, see [8,10]), giving us reasonable confidence in the numerical scheme employed. Currently therefore we are unable to offer a definitive explanation for this anomaly, although it may be that in the case studied here the maximum value of Le is not sufficiently high to recover the limiting case of $\mathrm{Le} \to \infty$. This would be consistent with experiment where at low undercoolings (i.e., $\Delta = 0.15$) the solidification of metals ($\mathrm{Le} \sim 10^4$) would still be expected to be under coupled thermosolutal control.

[1] G. P. Ivantsov, Dokl. Akad. Nauk SSSR **58**, 567 (1947).
[2] W. W. Mullins and R. F. Sekerka, J. Appl. Phys. **35**, 444 (1964).
[3] J. Lipton, W. Kurz, and R. Trivedi, Acta Metall. **35**, 957 (1987).
[4] D. A. Kessler, J. Koplik, and H. Levine, Adv. Phys. **37**, 255 (1988).
[5] J. R. Green, A. M. Mullis, and P. K. Jimack, Metall. Mater. Trans. A **38**, 1426 (2007).
[6] I. Loginova, G. Amberg, and J. Aagren, Acta Mater. **49**, 573 (2001).
[7] J. A. Warren and W. J. Boettinger, Acta Metall. Mater. **43**, 689 (1995).
[8] J. C. Ramirez and C. Beckermann, Acta Mater. **53**, 1721 (2005).
[9] C. W. Lan, Y. C. Chang, and C. J. Shih, Acta Mater. **51**, 1857 (2003).
[10] J. C. Ramirez, C. Beckermann, A. Karma, and H. J. Diepers, Phys. Rev. E **69**, 051607 (2004).
[11] A. Karma, Phys. Rev. Lett. **87**, 115701 (2001).
[12] J. Rosam, P. K. Jimack, and A. M. Mullis, Acta Mater. **56**, 4559 (2008).
[13] A. M. Mullis, Comput. Mater. Sci. **36**, 345 (2006).
[14] J. Rosam, Ph.D. thesis, University of Leeds, 2007.
[15] U. Trottenberg, C. Oosterlee, and A. Schuller, *Multigrid* (Academic, San Diego, 2001).
[16] A. Brandt, Math. Comput. **31**, 333 (1977).
[17] J. Rosam, P. K. Jimack, and A. M. Mullis, J. Comput. Phys. **225**, 1271 (2007).
[18] *Smithells Metals Reference Book*, 7th ed., edited by E. A. Brandes and G. B. Brook (Butterworth-Heinemann, London, 1992).
[19] X. Tong, C. Beckermann, A. Karma, and Q. Li, Phys. Rev. E **63**, 061601 (2001).
[20] X. J. Han, M. Chen, and Y. J. Lu, Int. J. Thermophys. **29**, 1408 (2008).
[21] S. E. Battersby, R. F. Cochrane, and A. M. Mullis, J. Mater. Sci. **34**, 2049 (1999).
[22] S. E. Battersby, R. F. Cochrane, and A. M. Mullis, J. Mater. Sci. **35**, 1365 (2000).